Journal of Alloys and Compounds 509 (2011) 2021–2030

Contents lists available at ScienceDirect

Journal of Alloys and Compounds

journal homepage: www.elsevier.com/locate/jallcom

Effect of alien cations on the growth mode and self-assemble fashion of ZnO nanostructures

Lihong Dong[a,b], Yang Liu[a,*], Yujiang Zhuo[a], Ying Chu[a,*], Yanping Wang[b]

[a] Department of Chemistry, Northeast Normal University, Changchun 130024, PR China
[b] Department of Chemistry, Tonghua Normal University, Tonghua 134002, PR China

ARTICLE INFO

Article history:
Received 22 July 2010
Received in revised form 16 October 2010
Accepted 22 October 2010
Available online 4 November 2010

Keywords:
Nanostructured materials
Semiconductors
Chemical synthesis
Crystal growth

ABSTRACT

In this paper, the effect of inorganic ions rather than organic additives on the morphology of ZnO nanostructures was investigated. A very simple synthesis system was designed, in which poly(vinyl pyrrolidone) (PVP) was selected as reference, several kinds of alien cations (Pb^{2+}, Cu^{2+}, and Co^{2+}) were introduced as additives to investigate their effect on the morphology of ZnO nanostructures systematically. The results indicated that alien cations influenced not only the growth mode but also the assembly fashion of the ZnO nanostructures. When the ionic radius of alien cations was close to that of Zn^{2+}, doped ZnO nanostructures were obtained. Furthermore, the introduction of alien cations made the photoluminescence properties of corresponding ZnO product greatly distinct from each other. Based on these results, several conclusions were drawn out and possible mechanism was put forward.

1. Introduction

Zinc oxide (ZnO), as an important functional oxide, is a direct wide band gap (3.37 eV) semiconducting and piezoelectric material with many useful properties, such as room temperature lasing, transparent electronics, power generation, photocatalysis, and sensitivity to gases [1–3]. Moreover, it is well known that not only the size but also the shape of metal oxide and semiconductor crystals has a profound effect on their properties [2]. In the last 10 years, numerous efforts have been made to explore various methods for the fabrication of ZnO nanostructures with different shapes and morphologies, such as chemical vapor deposition [4], chemical bath deposition [5], hydrothermal route [6], microemulsion approach [7], and solvothermal methods [8]. Meanwhile, a variety of influencing factors on the morphologies of ZnO nanostructures have also been investigated, for instance, temperature, concentration, reaction time, surfactant, polymer, and so on. However, to the best of our knowledge, there is no effort devoted to investigating the influence of alien ions as additives on the morphologies of ZnO nanostructures although many doped or composite ZnO nanostructures have been reported [9–12]. Whether alien ions have effect on the ZnO nanostructures? If they do, what effects will they make on the nanostructures? And how the effects are made? To make clear the above questions, we carried out a series of experiments to explore the influence of alien cations on the morphologies of ZnO nanostructures by adopting Pb^{2+}, Cu^{2+}, and Co^{2+} as the studied cases. The experimental results indicated that these alien cations had different effects on not only the growth mode but the assembly fashion of ZnO nanostructures. Some of them (Cu^{2+} and Co^{2+}) could dope into the lattice of ZnO to form doped ZnO nanostructures. Furthermore, the participation of different alien cations in the synthesis made the photoluminescence properties of corresponding ZnO product vary considerably.

2. Experimental details

The reagents used in our experiments were of analytical grade without further purification. The select of a suitable synthesis system was the prime task for us. What we investigated was the effect of alien cations on not only the growth mode but the self-assembly fashion of the final product, so the final product should be ZnO nanostructures assembled by nano-building-block. In addition, the synthesis system should be as simple as possible so as to there was minimal interference on the investigation of the effect of alien cations. After a series of trials, a simple system composed only of water, $Zn(CH_3COO)_2$ and NaOH was selected, which was hydrothermally treated in 50 mL Teflon-lined stainless steel autoclave at 120 °C for 12 h. And for comparison, experiments with poly(vinyl pyrrolidone) (PVP) (M_W = 30,000) as additive were also performed.

In the case of Pb^{2+} ions as alien cations, $Zn(CH_3COO)_2{\cdot}2H_2O$ (0.2194 g) was dissolved in 40 mL of distilled water to prepare the precursor solution with the concentration of 0.025 M. Then NaOH (0.8 g) and desired amount of $Pb(CH_3COO)_2{\cdot}3H_2O$ were added to

* Corresponding authors. Tel.: +86 431 85099320; fax: +86 431 5684009.
E-mail addresses: liuy732@nenu.edu.cn (Y. Liu), chuying@nenu.edu.cn (Y. Chu).

0925-8388/$ – see front matter © 2010 Elsevier B.V. All rights reserved.
doi:10.1016/j.jallcom.2010.10.127

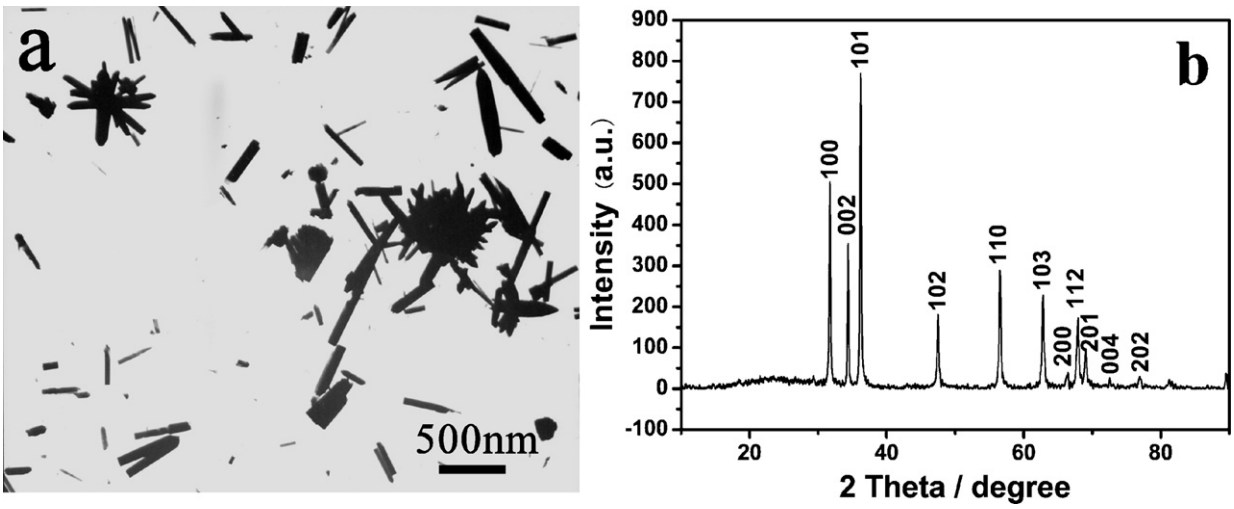

Fig. 1. (a) TEM image, (b) XRD pattern of the product obtained without any additive.

the precursor solution under constant stirring. After further stirring for 10 min, the solution was transferred into a 50 mL Teflon-lined stainless steel autoclave, followed by a hydrothermal treatment at 120 °C for 12 h. After reaction, the powder samples were collected, washed with distilled water, and dried at room temperature. The experiments with Cu^{2+} or Co^{2+} as alien cations were following the same procedure except corresponding salt [$Cu(CH_3COO)_2{\cdot}H_2O$ or $Co(CH_3COO)_2{\cdot}6H_2O$] was used.

The morphologies and structures of the synthesized product were characterized by Rigaku X-ray diffractometer (XRD) with Cu Kα radiation (λ = 1.5406 Å), transmission electron microscopy (TEM) (Hitachi H-800), and scanning electron microscopy (SEM)

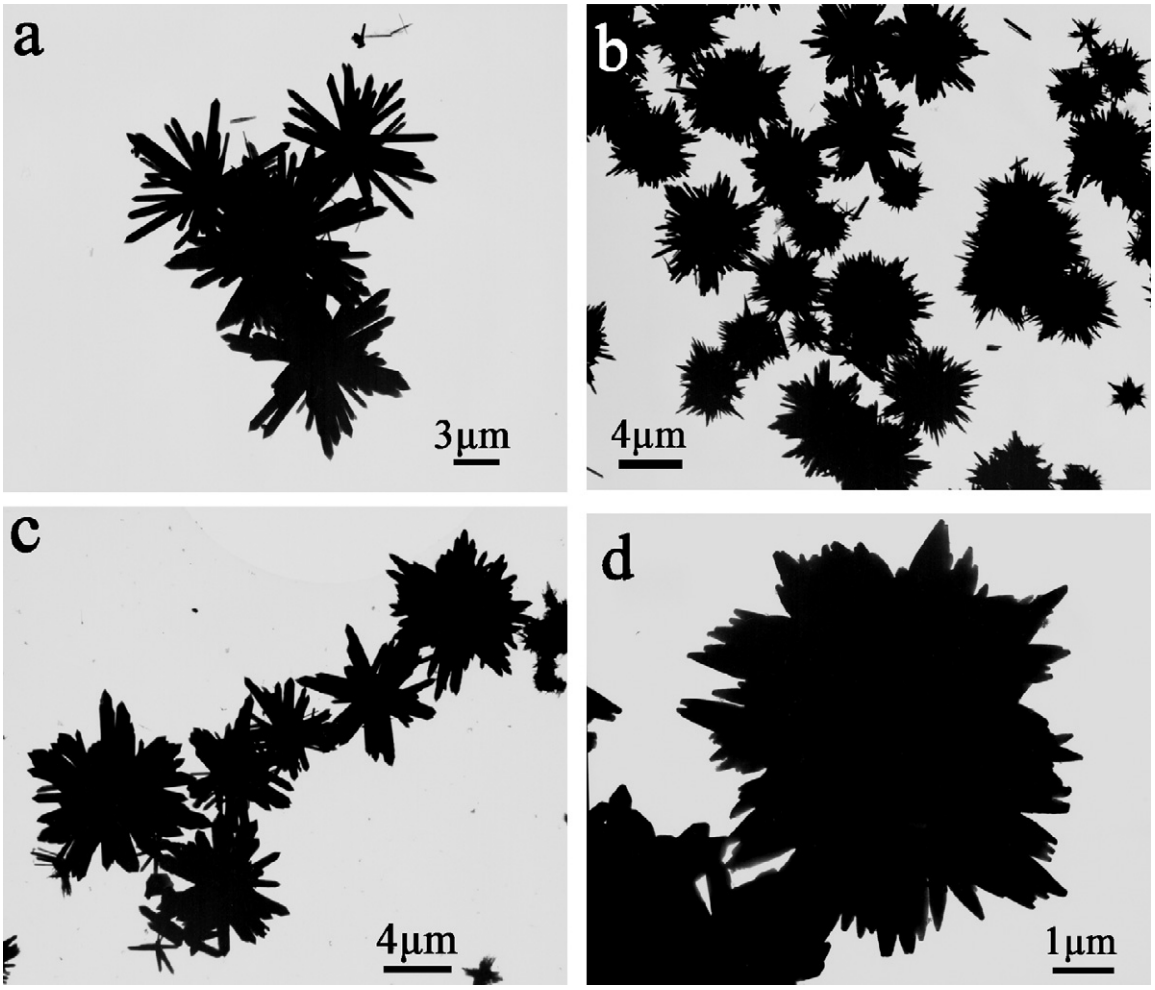

Fig. 2. TEM images of the products prepared with different Pb–Zn ratio: (a) 1:20, (b) 1:10, (c) 1:5, and (d) 1:2.5.

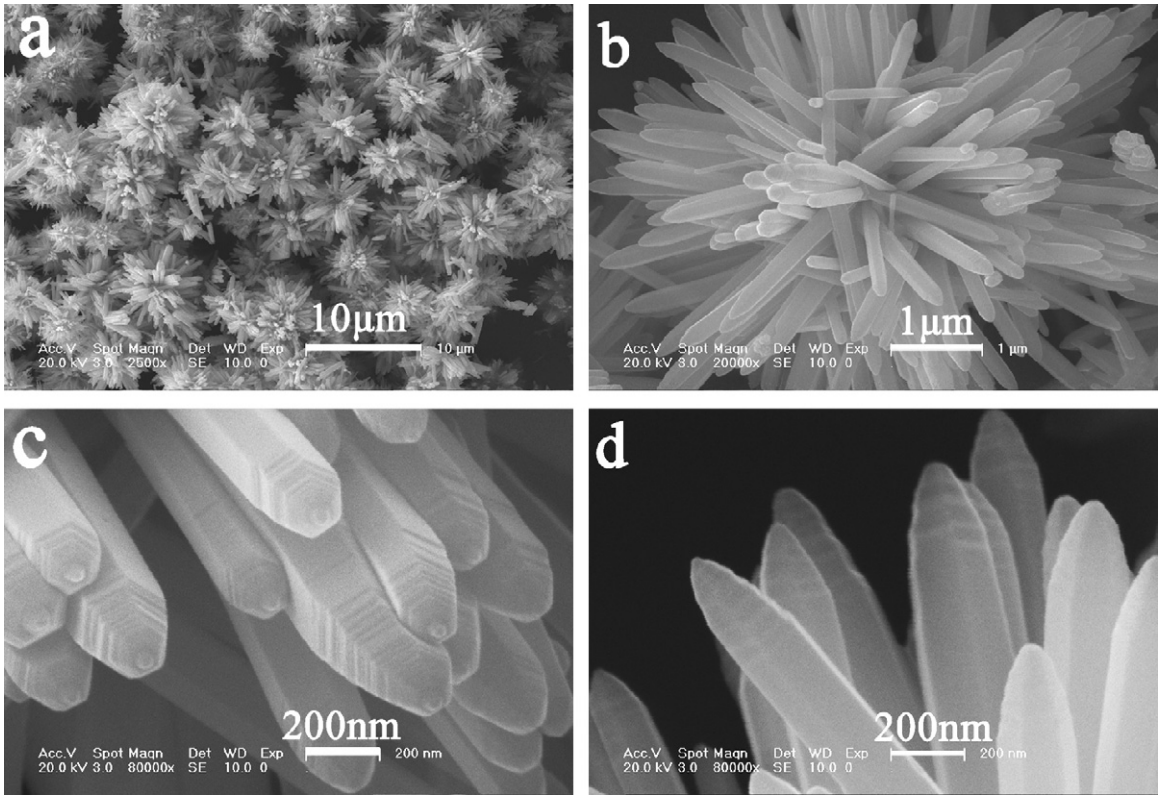

Fig. 3. SEM images of the product obtained with Pb–Zn ratio 1:10.

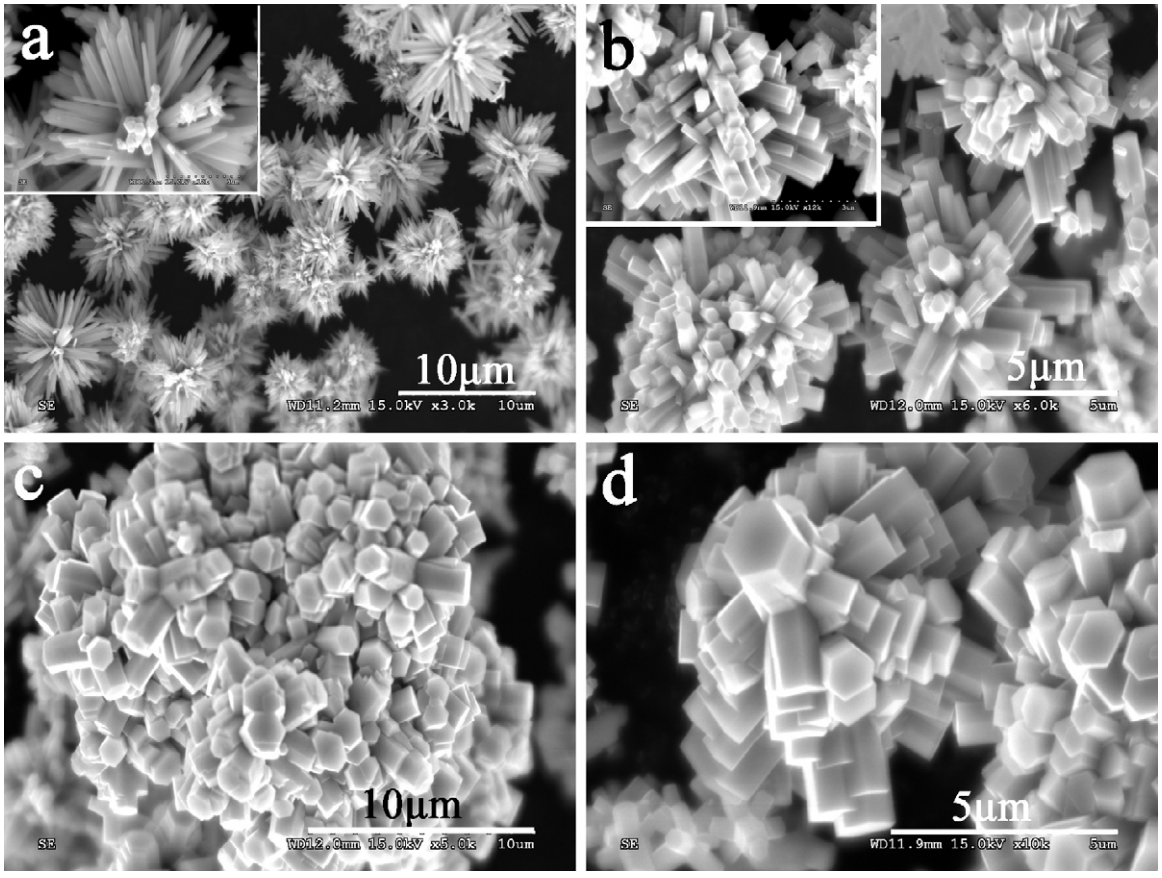

Fig. 4. ZnO nanostructures obtained with different amount of PVP: (a) 0.1 g, (b) 0.2 g, (c) and (d) 0.3 g.

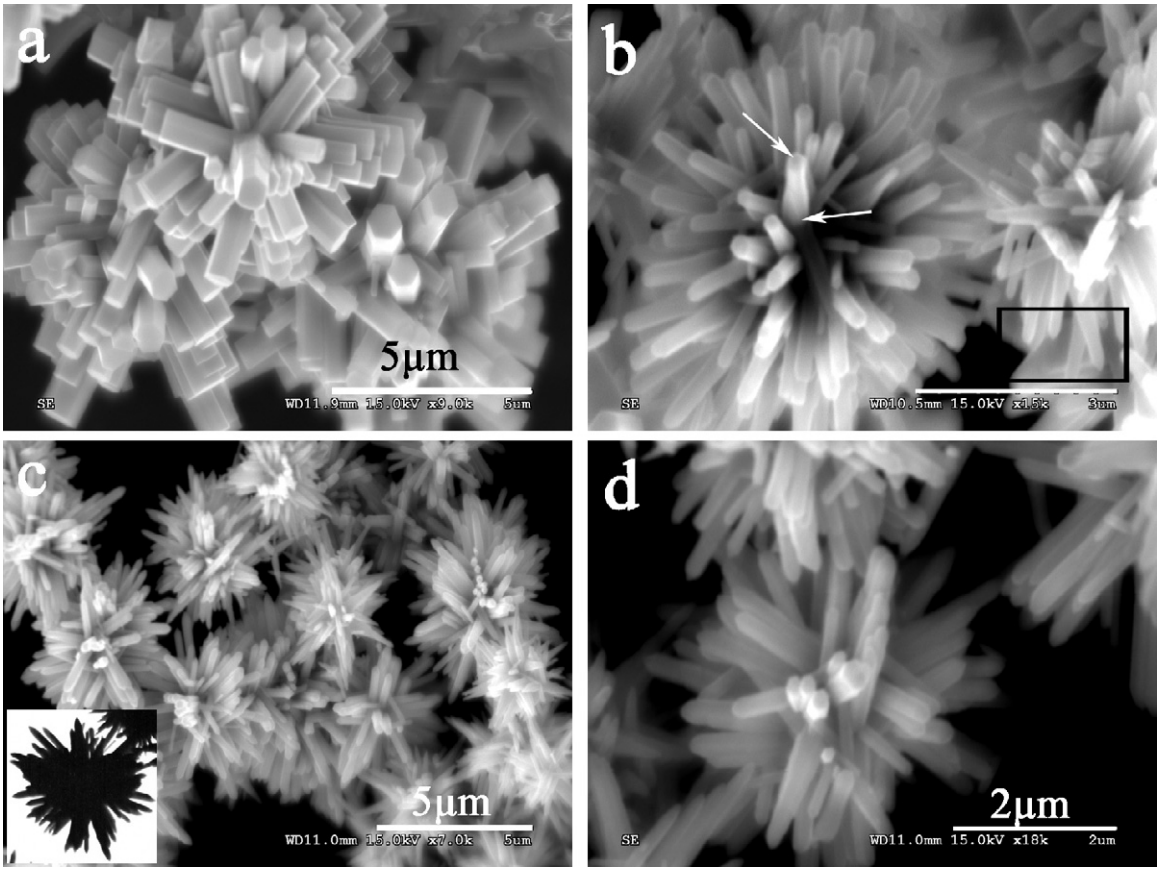

Fig. 5. SEM images of ZnO nanostructures obtained with 0.2 g PVP and different Pb-Zn ratio: (a) 1:20, (b) 1:10, (c) and (d) 1:5. The insert in (c) is a TEM image of a typical flower assembled by nanorods with sharp end. The scale bar in (b) represents 3 μm.

(JEOL, 7500B and HITACHI S-3000N). The photoluminescence (PL) measurement was performed on a HR-800 LabRam confocal Raman microscope made by JY Company, excited by the 325 nm line of a continuous He–Cd laser at room temperature.

3. Results and discussion

The product of control experiment without any additive was composed of nanorods and flower-like nanostructures assembled by nanorods, as shown in Fig. 1a. All the nanorods (free or assembled) were not uniform both in length and diameter. Moreover, the end of nanorod was either sharp or flat. The phase composition and phase structure of the as-obtained sample were examined by XRD. As shown in Fig. 1b, all of the peaks can be readily indexed as hexagonal wurtzite ZnO (JCPDS card No. 36-1451, $a = 0.325$ nm and $c = 0.521$ nm) with high crystallinity. No obvious impurity phase was found.

However, when a certain amount of $Pb(CH_3COO)_2$ was introduced into the synthesis system, almost all the product was flower-like nanostructures assembled by nanorods with sharp end. The typical TEM images corresponding to Pb–Zn ratio of 1:20, 1:10, 1:5 and 1:2.5 are shown in Fig. 2a–d, respectively. It can be seen that the flower has an average size of about 4–8 μm with sharp ends observable in every nanorods, and the flowers obtained with different Pb–Zn ratios showed unnoticeable difference. These observations manifested the impact of Pb^{2+} on the morphology of ZnO nanostructures.

The product with Pb–Zn ratio of 1:10 was further characterized by SEM, as shown in Fig. 3a, and large scale of uniform dandelion-like nanostructures assembled by nanorods with sharp ends can be clearly observed. Fig. 3b shows the magnified SEM image of a typical dandelion-like nanostructure. The size of the whole flower is about 5 μm, and the building-blocks, nanorods, are 200 nm in diameter and 1–2 μm in length. Well-defined edges of the nanorods with hexagonal cross section can be clearly seen in Fig. 3c, providing strong evidence that the single nanorod grows along the *c*-axis direction [13]. The six side surfaces are very smooth whereas the end part appears to be a layer-stack structure that looks like screw or tower; such phenomenon means that the end part is the growth point of the nanorods. Moreover, the main body of the nanorod is consistent in diameter but the end becomes thinner eventually (Figs. 3b and d), which further confirms the growth direction along the *c*-axis. Therefore, the existence of Pb^{2+} ions not only contributes to the formation of the flower-like self-assembly nanostructures but also facilitates the one-dimensional growth predominance along *c*-axis, which results in the formation of nanorods with smaller diameter and sharper end.

To shed light on the action mechanism of Pb^{2+} ions, a common structure-directing agent, PVP, was introduced into synthesis system for comparison. PVP, as a kind of non-ionic surfactant, contains nitrogen (N) and oxygen (O) atoms in its pyrrolidone ring. From the viewpoint of the molecular structures, the oxygen atom is more electronegative than nitrogen atom and it is expected that the negative charge on PVP prefers to reside on oxygen atom. The partial positive charge on the nitrogen atom and the partial negative charge on the oxygen atom can behave as electron acceptor and donor, respectively [14,15]. Hence, the PVP molecules may exist in two resonance structures [16]. In polar circumstance, such as in water, the inner molecular acylamino bond is intent to transform to hydrophilic $-N^{+}{=}C{-}O^{-}$ bond. Together with the hydrophilic $C{-}O^{-}$

bond, the hydrophobic C–C bond makes the PVP an alternate surfactant and the PVP molecules can adsorb selectively on special crystal faces during crystal growth. So PVP is used extensively to control anisotropic growth of crystal including the fabrication of nanocrystals, ZnO hexagonal nanoprisms have been synthesized under the assistance of PVP via a microemulsion route, in which the PVP adsorbed selectively on the (0 0 0 1) faces of ZnO [16]. In this paper, different amount of PVP was used firstly to ascertain which crystal faces were adsorbed preferentially, and the experimental results are shown in Fig. 4. In Fig. 4a, a SEM image of the product obtained with the PVP amount of 0.1 g, uniform flower-like nanostructures assembled by nanorods with sharp end are essentially the exclusive product. When the amount of PVP increased to 0.2 g, the product was still flower-like nanostructures assembled by nanorods, but the end became flat as shown in Fig. 4b. The insert is a side view of one flower, in which flat end can be clearly seen. Further increasing PVP amount to 0.3 g, sphere-like or hemisphere-like nanostructures were the main products, and the building blocks of these nanostructures were well defined hexagonal nanoprisms or nanoplates as shown in Figs. 4c and d. Based on the above results, three conclusions can be obtained. Firstly, in all the cases, hexagonal cross section of the building blocks is clear at a glance, suggesting the growth direction of the nanorod or nanoprism is also ⟨0 0 0 1⟩. Secondly, with the increase of PVP amount, the end part of building block transforms from sharp to flat, the length becomes shorter and shorter, and the diameter gets larger and larger. All of these indicate that the PVP molecules adsorbed selectively on (0 0 0 1) faces of ZnO, which limited the growth along ⟨0 0 0 1⟩ direction. So, for the fabrication of ZnO nanocrystals, PVP always adsorbs selectively on (0 0 0 1) faces in not only microemulsion route but hydrothermal method. Finally, the existence of PVP is in favor of the formation of flower-like self-assemble nanostructures compared with the control experiment stated previously, which may be resulted from the steric hindrance of PVP adsorbed on the surfaces of ZnO nanorods (or nanorprisms) as well as the linear structure and multiple coordinating sites of PVP molecules [17].

After investigating the role of PVP, we chose the case of 0.2 g PVP as the testing system, into which $Pb(CH_3COO)_2$ with different Pb–Zn ratio (1:20, 1:10, and 1:5) was added, under otherwise the same conditions. No different morphologies other than flower were obtained, as presented in Fig. 5. When the Pb–Zn ratio was 1:20, as depicted in Fig. 5a, the end of the nanorods was still flat as same as that obtained without Pb^{2+} ions. Whereas, in the case of Pb–Zn ratio 1:10, the end of some nanorods became sharp as indicated by the black rectangle in Fig. 5b. Although the others owned flat end, the diameter of the top was obviously smaller than that of the bottom as indicated by the white arrows. Continuous increase of the Pb–Zn ratio to 1:5 resulted in the complete transformation from flat into sharp ends, as shown in Figs. 5c and d. The insert in Fig. 5c is a TEM image of a typical flower assembled by nanorods with sharp end. These results further confirm the argument above that Pb^{2+} ions facilitate the one-dimensional growth predominance along *c*-axis, which means that Pb^{2+} ions adsorb selectively on the faces parallel to ⟨0 0 0 1⟩ direction. It has been reported that inorganic ions can adsorb on the surfaces of metal oxide [18–21], and density functional theory also verified this viewpoint [22]. The predominant faces to be adsorbed should depend on different synthesis system, specific ions and metal oxide. In present case, Pb^{2+} ions adsorbed selectively on the faces parallel to ⟨0 0 0 1⟩ direction, leading to a competition between Pb^{2+} ions and PVP molecules. When the amount of Pb^{2+} ions was little, such as a Pb-Zn ratio of 1:20, the adsorption of PVP molecules on (0 0 0 1) faces had the upper hand, so the end of the nanorods was flat. Whereas, when the amount of Pb^{2+} ions exceeded a certain value (for instance, Pb–Zn = 1:5), the adsorption of Pb^{2+} ions on the faces parallel to ⟨0 0 0 1⟩ direction was superior. Therefore, the growth along the ⟨0 0 0 1⟩ direction was promoted greatly, resulting in sharp end of all the nanorods.

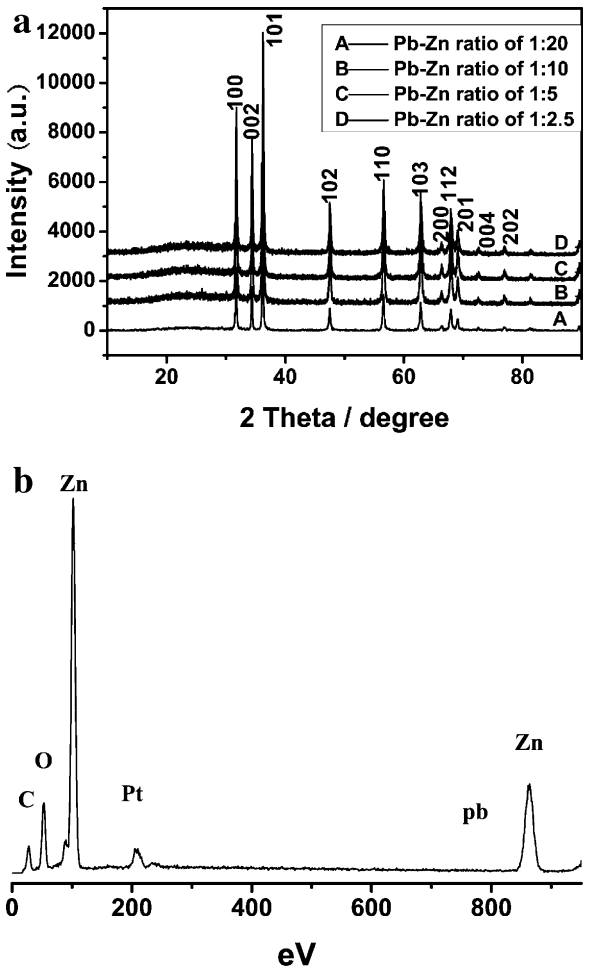

Fig. 6. (a) XRD patterns of the ZnO nanostructures obtained with different Pb–Zn ratio, (b) EDS patterns of the ZnO nanostructures obtained with Pb–Zn ratio of 1:10.

In Fig. 6a, the XRD patterns from the bottom to the top are corresponding to the products with Pb–Zn ratio of 1:20, 1:10, 1:5 and 1:2.5, respectively. All of the reflection peaks of the products can be indexed as pure hexagonal ZnO, and no characteristic diffraction peaks from other phases or impurities (such as PbO_2, Pb_3O_4) are detected, indicating the high purity of the product. To get to know whether the Pb was doped into the lattice of ZnO nanostructures, the product of Pb–Zn ratio of 1:10 was investigated as representative by inductively coupled plasma (ICP) atomic emission spectroscopy and electron dispersive spectrum (EDS) (Fig. 6b). The measurement result of the former is 0.5% (molar ratio), and the latter is 0.43%. For the initial dosage was relative high, such small content in the final product allowed us to believe that the Pb element detected by ICP and EDS should come from those adsorbed on the surface of the ZnO nanostructures and Pb did not dope into the ZnO lattice. The great difference of ionic radius between Zn^{2+} and Pb^{2+} (Zn: 74 pm, Pb: 119 pm) should contribute to this phenomenon. Of course, more in-depth studies are necessary for further understanding the exact reason.

What about Cu^{2+}? The ionic radius of Cu^{2+} is 73 pm, which is very close to that of Zn^{2+}. Can Cu element dope into ZnO lattice? And what influence on the morphology of the ZnO nanostructures can be made by the introduction of Cu^{2+} ions? So a series of experiments were carried out by replacing Pb^{2+} with Cu^{2+}, and the results are shown in Figs. 7 and 8. Fig. 7a is a panoramic SEM image of the

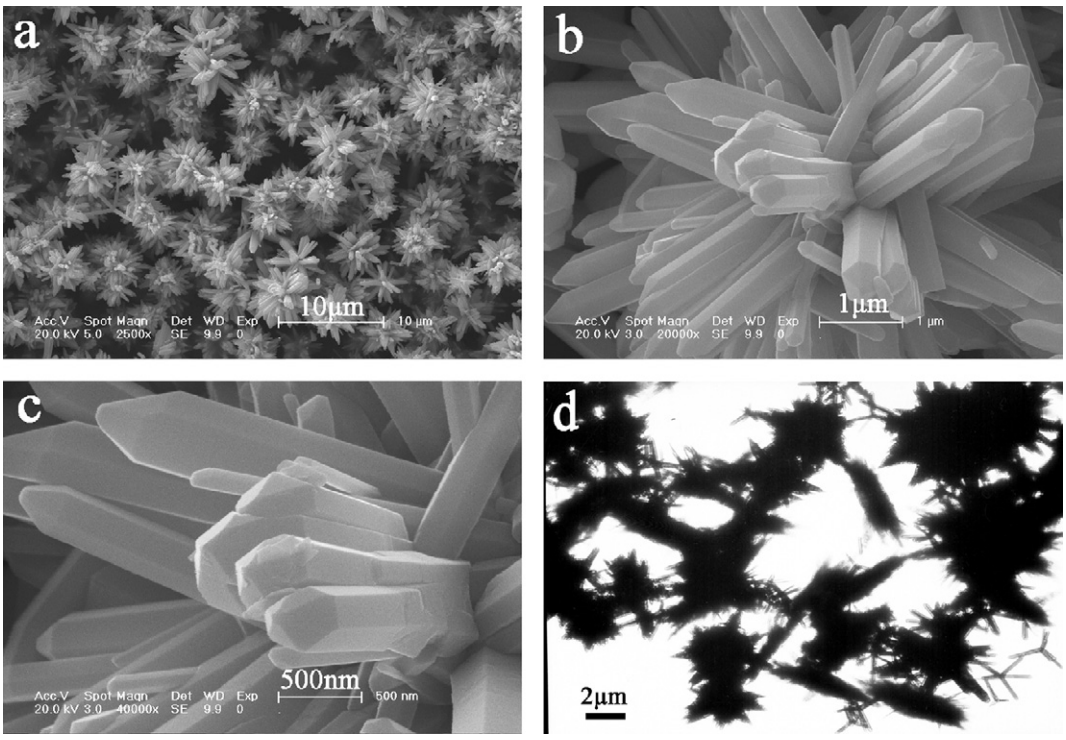

Fig. 7. (a)–(c) SEM images with different magnification of the product obtained with Cu–Zn ratio of 1:20, (d) TEM image of the product obtained with Cu–Zn ratio of 1:5.

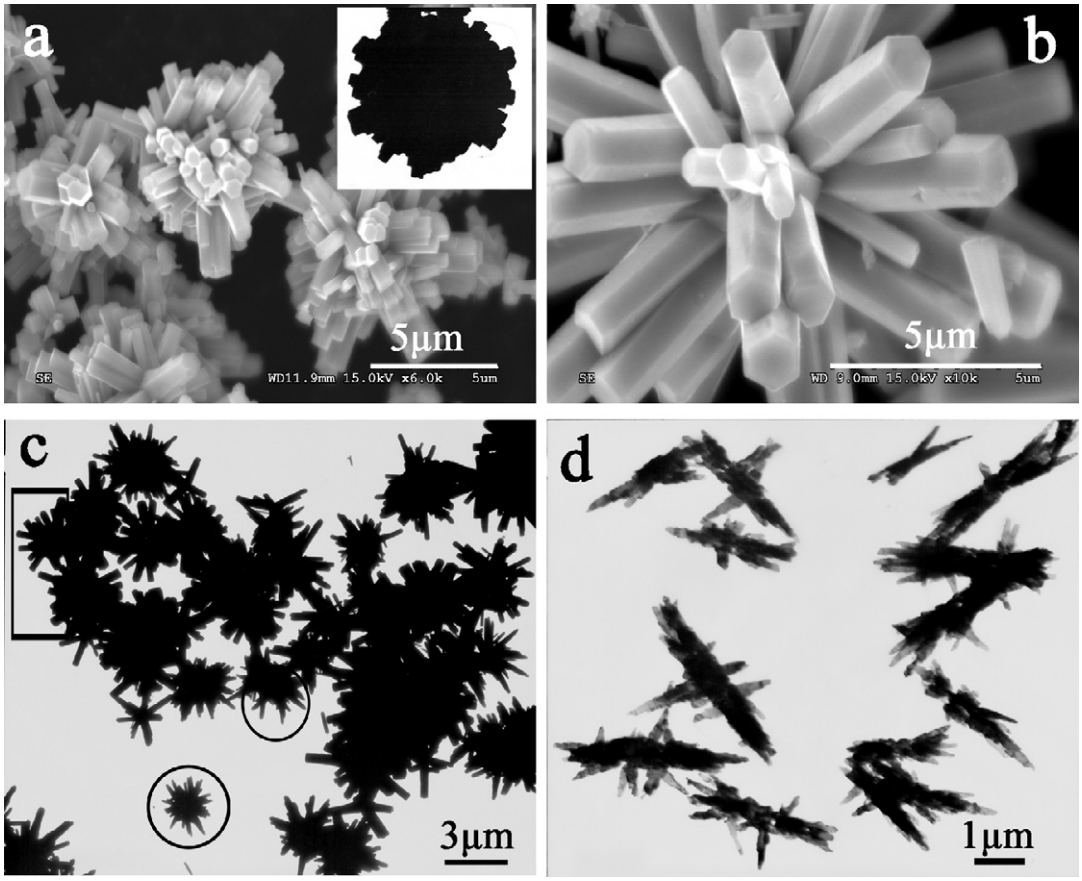

Fig. 8. (a) and (b) SEM images of the product obtained with 0.2 g PVP and Cu–Zn ratio of 1:20, (c) TEM image of the product obtained with 0.2 g PVP and Cu–Zn ratio of 1:10, (d) TEM image of the product obtained with 0.2 g PVP and Cu–Zn ratio of 1:5.

product obtained with Cu–Zn ratio of 1:20 without PVP, flower-like nanostructures composed of nanorods are still the exclusive product, and the nanorods also possess hexagonal cross section, well-defined facets and edges as well as sharp end as shown in Fig. 7b. But a closer inspection of the magnified image (Fig. 7c) reveals that the nanorods are somewhat different from those in the case of Pb^{2+} ions. First of all, although the end part is also sharp, the surface is very smooth (the surface of end part in the case of Pb is matte and like tower); the boundaries between adjacent two faces at the end part are clearly visible (there was no boundary found in the case of Pb); and the whole shape of the nanorod looks more like a pencil than a tower. Secondly, the diameter of these nanorods is around 500 nm compared to *ca.* 200 nm in the case of Pb. When the Cu–Zn ratio was up to 1:10, there was no obvious change observed, so the related data is not shown here. Further increase of the Cu–Zn ratio to 1:5 led to the appearance of some bundle-like nanostructures as shown in Fig. 7d. These results reveal that the Cu^{2+} ions are also in favor of the self-assembly of flower-like fashion, but this kind of effect turns weak when the amount of the Cu^{2+} ions reaches a certain value, leading to the formation of bundle-like products. Otherwise, adsorbing ability of the Cu^{2+} ions on the faces parallel to ⟨0 0 0 1⟩ direction is not as strong as Pb^{2+} ions (or other faces were adsorbed by Cu^{2+} ions?), which results in the nanorods obtained much thicker than those obtained with Pb^{2+} ions.

To ascertain which faces are really adsorbed by Cu^{2+} ions, PVP was adopted as the reference again. The dosage of PVP was still 0.2 g in order to make a paparallel comparison with the case of Pb conveniently. When the Cu–Zn ratio was 1:20, the product was sphere-like flowers composed of microprism or microrods as shown in Figs. 8a and b. The end of all the building blocks was flat with hexagonal crossing section, indicating that Cu^{2+} ions made little effect on the adsorption of PVP on (0 0 0 1) faces in this case. When the Cu–Zn ratio was 1:10, the product consisted of flowers composed of nanorods with flat or sharp end (Fig. 8c), and statistical result during the TEM investigation showed that flat end was the majority, which means Cu^{2+} ions also adsorb on the faces parallel to ⟨0 0 0 1⟩ direction, leading to the formation of some nanorods with sharp end. But their ability of competition with PVP is inferior to that of Pb^{2+} ions, so the flat-ended product is still the majority. When more Cu^{2+} ions, such as Cu–Zn ratio of 1:5, were used, the product was not yet flowers but bundle-like nanostructures as shown in Fig. 8d, suggesting that Cu^{2+} ions further changed the self-assembly fashion when its amount was above a threshold value even if the PVP coexisted, which is in agreement with the case without PVP.

The products obtained with Cu^{2+} ions were further characterized by XRD (Fig. 9). When the Cu–Zn ratio was 1:20, the product was pure hexagonal ZnO (Fig. 9a-A). When the Cu–Zn ratio was increased to 1:10, a small impurity peak indexed to cubic CuO appeared as the asterisk indicated (Fig. 9a-B). Further increase of Cu–Zn ratio to 1:5 led to the presence of more CuO as shown in Fig. 9a-C. The product obtained with Cu–Zn ratio of 1:20 was further investigated by EDS (Fig. 9b), and the result that a Cu–Zn ratio of 0.0415 means the Cu element had doped into the ZnO lattice, and doping level is very high compared with the initial Cu amount of 0.05. Thus, the experimental phenomena mentioned above could be explained as follows: when the Cu–Zn ratio was small (1:20), almost all of the Cu^{2+} ions took part in the doping and there were few dissociative Cu^{2+} ions in the system, so there was no obvious influence on the PVP adsorption; when the Cu–Zn ratio is augmented (1:10), dissociative Cu^{2+} ions began to emerge, some of them adsorbed on the faces parallel to ⟨0 0 0 1⟩ direction resulting in the formation of nanorods with sharp end, but the adsorption on the faces parallel to ⟨0 0 0 1⟩ direction was not entire owing to the transformation of some Cu^{2+} ions into CuO, so the main nanorods

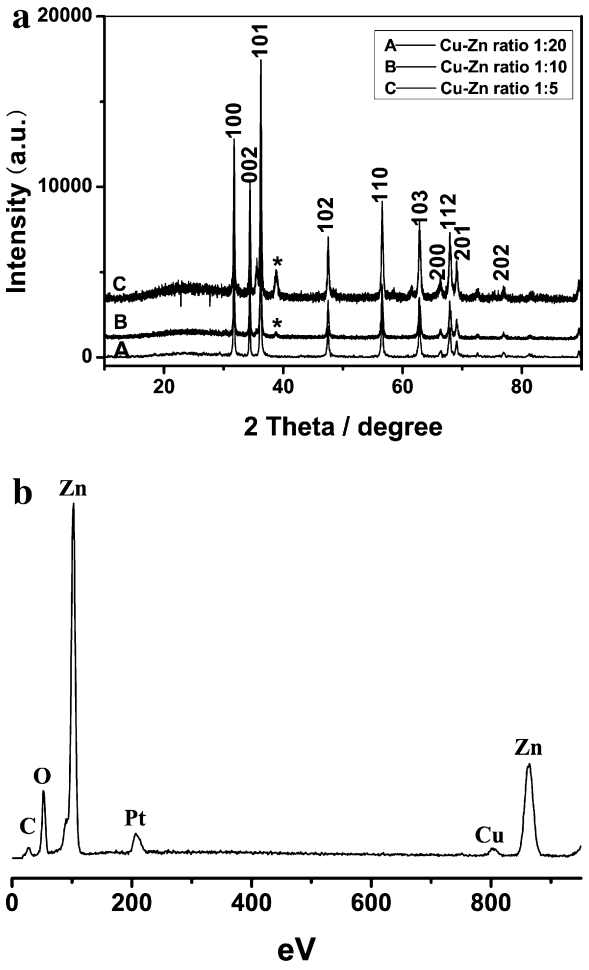

Fig. 9. (a) The XRD patterns of the product obtained with different Cu–Zn ratio, (b) EDS pattern of the product obtained with Cu–Zn ratio 1:5.

were flat, namely the PVP adsorption was affected slightly; when too much Cu^{2+} ions were introduced, more CuO impurities were formed, and the function of PVP was affected seriously in both adsorption and assembly, so the product was not still the flower-like structures as before.

Diluted magnetic semiconductors have attracted considerable attention in the past few years due to their promising applications in spintronic devices [23]. Many Co doped ZnO nanostructures have been obtained by thermal chemical vapor deposition method [24], ion-implanted methods [25], coprecipitation technology [26], hydrothermal route [27], and so forth. Herein, we would like to know if the Co element could dope into ZnO nanostructures because Co^{2+} ionic radius (74.5 pm) is nearer to Zn^{2+} (74 pm) than Cu^{2+} ions (73 pm). In addition, what we were more curious about was that whether the Co^{2+} ions also took effect on the morphology of final product. So a series of experiments were conducted and some interesting results were obtained. First of all, the introduction of Co^{2+} ions also had effect on the morphology of the products whether the PVP existed or not, the corresponding TEM and SEM images are shown in Fig. 10. Fig. 10a is a TEM image of the product obtained with 0.2 g PVP and Co–Zn ratio of 1:20, flower-like structures were still the majority, but the number of nanorods in one flower decreased, some flowers were composed of only six or three nanorods as indicated by circle and rectangle, respectively. In addition, the end of most nanorods was flat. When the Co–Zn ratio was increased to 1:10, the number of nanorods in one flower further reduced as shown in Fig. 10b, and the end of many nanorods became sharp. On the other hand, lots of impurity, cubic nanopar-

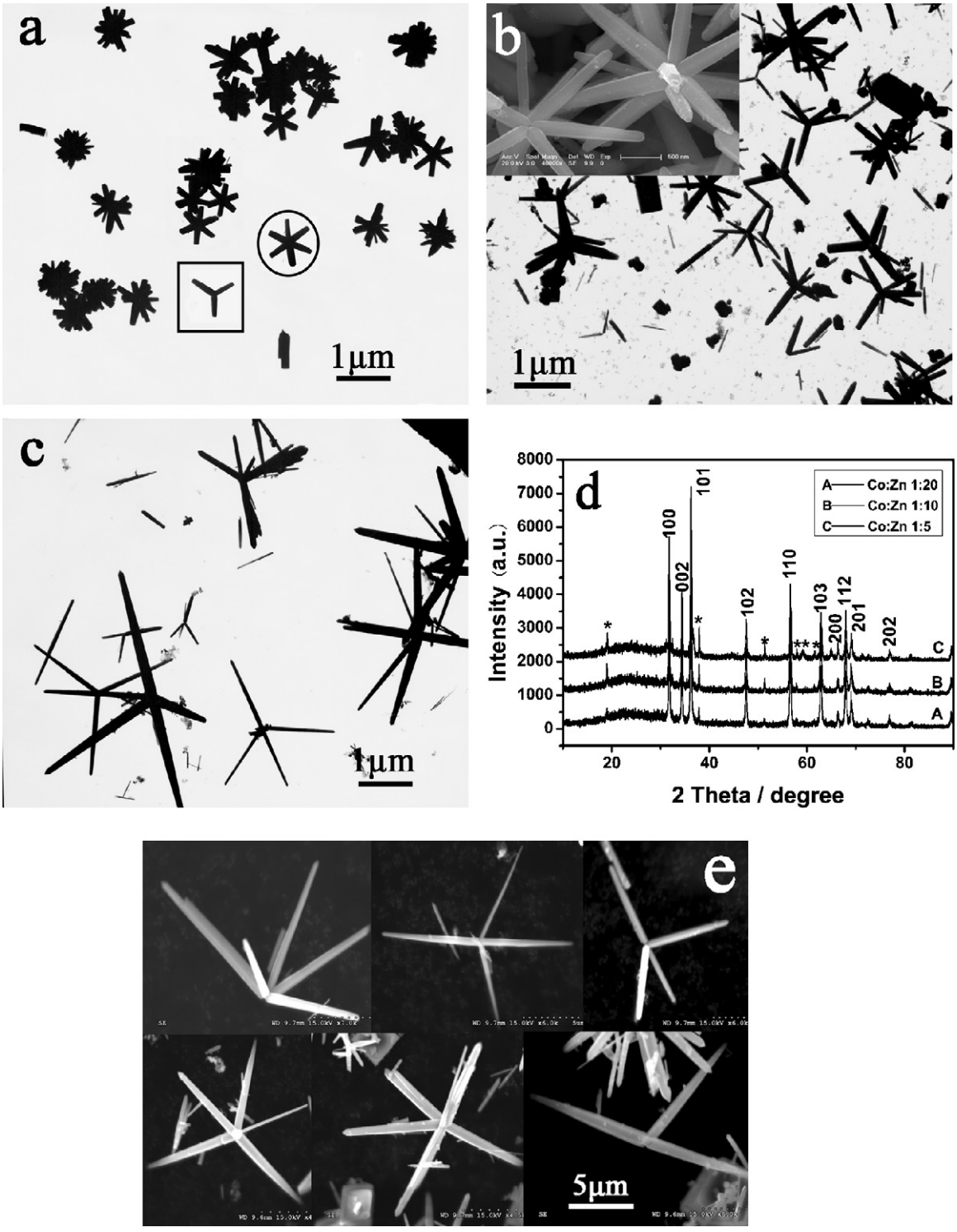

Fig. 10. TEM images of the product obtained with 0.2 g PVP and different Co–Zn ratio: (a) 1:20, (b) 1:10, (c) 1:5, (d) XRD pattern of the product obtained with different Co–Zn ratio, (e) SEM images of the product obtained without PVP and Co–Zn ratio of 1:5.

ticles, could be found. So a conclusion could be made that the Co^{2+} ions also adsorb on the faces parallel to the ⟨0 0 0 1⟩ direction, but impurity is easy to form in the present synthesis system. Continuous increase of the Co^{2+} ions must lead to more nanorods with sharp end and more impurity, and the experiment with Co–Zn ratio of 1:5 verified our speculation as shown in Fig. 10c: the number of the nanorods in one flower further decreased, such morphology is often called multi-arm in many reports. The products obtained with different Co–Zn ratio and without PVP were similar with those obtained with PVP, so we only show the case of Co–Zn ratio of 1:5 in Fig. 10e. Besides multi-arm composed with different number of nanorods, there was still large quantity of impurity. The existence of impurity is also confirmed by XRD investigation (Fig. 10d), which should be indexed to $Co(OH)_2$. EDS measurement of Co–Zn ratio 1:20 indicated that the amount of Co in ZnO nanostructures was about 3.92% (molar ratio), which means that Co element can dope into ZnO lattice. Thus, the Co^{2+} ions also made effect on both the growth mode and the assembly of ZnO nanorods.

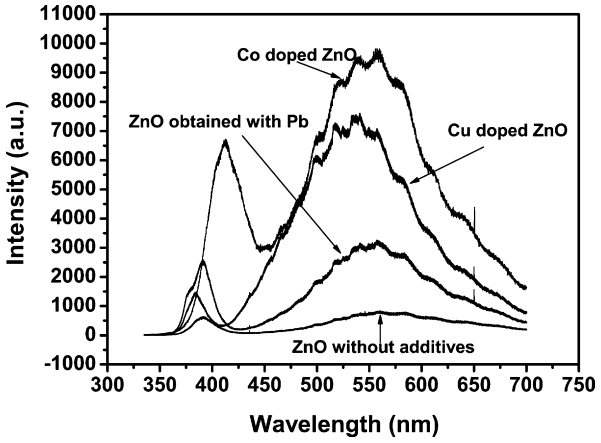

Fig. 11. The PL spectra of the ZnO nanotructures obtained with alien cation–Zn of 1:20.

We suggested the different effect of alien cations on the assembly fashion should also result from their different adsorption. In all the cases, ZnO nuclei formed initially, and then these ZnO nuclei congregated to form globose nanocrystals which were adsorbed by alien cations. These cations would bind with the O^{2-} on the polar (0 0 0 −1) planes of ZnO (it is well known that ZnO is a polar crystal, which can be described as a number of tetrahedrally coordinated O^{2-} and Zn^{2+} ions stacking alternatively along the *c* axis), so ZnO preferred to grow along the ⟨0 0 0 1⟩ axis to form nanorods with the assistance of alien cations adsorption and flower-like nanostructure formed finally. In the case of Pb, the amount of Pb^{2+} ions on the surface of ZnO nanocrystals was large, so the number of nanorods in one final flower was large. Whereas in the case of Cu, most of Cu^{2+} ions doped into ZnO, the amount of Cu^{2+} ions on the surface of ZnO nanocrystals was relative small, so the number of nanorods in one final flower was less than that of Pb. With regard to Co^{2+} ions, they not only doped into ZnO lattice but also were highly susceptible to form $Co(OH)_2$ in the basic medium, so the amount on the surface of ZnO nanocrystals further decreased, multi-arms came into being accordingly. However, direct evidence for this hypothesis requires further study and work is underway.

Summing up all of the above discussion, several conclusions were drawn out as follows. Firstly, alien cations can make great effect on the morphology of ZnO nanostructures in not only the assembly fashion but the growth mode of building blocks. Secondly, cations usually realize these effects by adsorbing on the faces parallel to the ⟨0 0 0 1⟩ direction. But the absorbability depends on different kinds of cations, and in present cases, the strongest one should be Pb^{2+} ion because it has larger ionic radius, which limited its doping into ZnO lattice, and lead oxide or other lead compounds cannot form in such synthesis system. These two factors ensure more free Pb^{2+} ions in solution. Thirdly, when the ionic radius of alien cations, such as Cu^{2+} and Co^{2+}, is similar to that of Zn^{2+}, they can dope into the lattice of ZnO to form doped ZnO nanostructures, but the amount of alien cations should be limited in a certain range to avoid the formation of impurity. However, there is still so much we do not know about the effect of alien cations, for example the exact interpretation for the formation of multi-arms resulted from the existence of Co ions, the difference between Co and Cu even if they are very similar in both ionic radius and chemical valence, and how about the other alien cations, so more in-depth studies are necessary to make further understand.

In order to avoid the interference of impurity, we only investigated the PL properties of the ZnO nanotructures obtained with alien cation–Zn of 1:20, and the results are shown in Fig. 11. These PL spectra all exhibit two emission bands located at about 380 and 550 nm, respectively, which is consistent with literature [28]. The UV band emission can be assigned to the emission from a free exciton under low excitation intensity, and the peaks in the green band possibly originate from the electron transition from the level of the ionized oxygen vacancies to the valence band [29]. The intensity of both UV and defect-related green emission increases by the introduction of alien cations. The increase brought by Pb is larger than that brought by Cu in UV emission, whereas in green emission, the increase brought by Cu is much larger than that of Pb. As for Co, the intensity in both emissions is the highest, and the UV emission shows slightly red shift. Overall, the increase of green emission is more than that in UV emission, indicating that lots of oxygen vacancies or interstitial Zn centers formed when alien cations were introduced. And the relative higher increase aroused by Cu and Co further confirms that they have doped into ZnO lattice, which led to more lattice defect. The above results also reveal that the emission spectra of the products synthesized under different conditions are dramatically different from each other, verifying that the optical properties of ZnO crystals are very sensitive to the morphology and preparation conditions.

4. Conclusions

By adopting a very simple fabrication system and comparing with surfactant PVP, the effect of several alien cations (Pb^{2+}, Cu^{2+} and Co^{2+}) on the morphology of ZnO nanostructures was investigated. The results revealed that these cations could adsorb on the faces parallel to the ⟨0 0 0 1⟩ direction of ZnO in various degrees, leading to the formation of nanorods with sharp or flat end. Also, these cations played an important roles in the self-assembly fashion of the nanorods to form flower-like nanostructures. When the ionic radius of the alien cations is close to that of Zn cation, they would dope into the ZnO lattice in a certain concentration range. Moreover, the participation of alien cation in the synthesis brought about obvious variety of photoluminescence property. Therefore, it is believed that the introduction of alien cations is an effective means to modulate the growth mode, self-assembly fashion and property of nanotructures, which has the advantage that no any organic additive is needed, and opens a new "window" for the fabrication of nanostructures with various morphologies as well as the modulation of property.

Acknowledgements

This work was supported by the Natural Science Fund of China (Nos. 20573017 and 20803008), 11th Five-Year Plan in science and technology of the Education Department of Jilin Province (2009-266), and Analysis and Testing Foundation of Northeast Normal University.

References

[1] Z.L. Wang, J.H. Song, Science 312 (2006) 242–246.
[2] A. Mclaren, T. Valdes-Solis, G.Q. Li, S.C. Tsang, J. Am. Chem. Soc. 131 (2009) 12540–12541.
[3] Q.F. Zhang, C.S. Dandeneau, X.Y. Zhou, G.Z. Cao, Adv. Mater. 21 (2009) 4087–4108.
[4] S.L. Wang, X. Jia, P. Jiang, H. Fang, W.H. Tang, J. Alloys Compd. 502 (2010) 118–122.
[5] X.H. Liu, M. Afzaal, K. Ramasamy, P. O'Brien, J. Akhtar, J. Am. Chem. Soc. 131 (2009) 15106–15107.
[6] S.H. Hua, Y.C. Chenb, C.C. Hwangb, C.H. Pengc, D.C. Gonga, J. Alloys Compd. 500 (2010) L17–L21.
[7] L. Gao, Y.L. Ji, H.B. Xu, P. Simon, Z.Y. Wu, J. Am. Chem. Soc. 124 (2002) 14864–14865.
[8] Z.G. Jia, L.H. Yue, Y.F. Zheng, Z.D. Xu, Mater. Chem. Phys. 107 (2008) 137–141.
[9] X.Y. Xu, C.B. Cao, J. Alloys Compd. 501 (2010) 265–268.
[10] T.K. Jia, W.M. Wang, F. Long, Z.Y. Fu, H. Wang, Q.J. Zhang, J. Alloys Compd. 484 (2009) 410–415.

[11] Y.L. Zuo, S.H. Ge, Z.Q. Chen, L. Zhang, X.Y. Zhou, S.M. Yan, J. Alloys Compd. 470 (2009) 47–50.
[12] T. Chen, G.Z. Xing, Z. Zhang, H.Y. Chen, T. Wu, Nanotechnology 19 (2008) 435711.
[13] Y.H. Tong, Y.C. Liu, C.L. Shao, Y.X. Liu, C.S. Xu, J.Y. Zhang, Y.M. Lu, D.Z. Shen, X.W. Fan, J. Phys. Chem. B 110 (2006) 14714–14718.
[14] M.M. Robert, M.K. Jonathan, Tetrahedron Lett. 9 (1966) 891–896.
[15] M.C.R. Symons, J.M. Harvey, S.E. Jackson, J. Chem. Soc. Faraday Trans. 1 76 (1980) 256–265.
[16] X.M. Sui, Y.C. Liu, C.L. Shao, Y.X. Liu, C.S. Xu, Chem. Phys. Lett. 424 (2006) 340–344.
[17] O. Spalla, M. Nabavi, J. Minter, B. Cabane, Colloid Polym. Sci. 274 (1996) 555–567.
[18] A.R. Krotan, R. Hull, R.L. Opila, M.G. Bawendi, M.L. Steigerwald, P.J. Carrol, L.E. Brus, J. Am. Chem. Soc. 112 (1990) 1327–1332.
[19] L. Gunneriusson, D. Baxter, H. Emteborg, J. Colloid Interface Sci. 169 (1995) 262–266.
[20] C. Ludwig, P.W. Schindler, J. Colloid Interface Sci. 169 (1995) 284–290.
[21] E.C. Hao, B. Yang, S. Yu, M.Y. Gao, J.C. Shen, Chem. Mater. 9 (1997) 1598–1600.
[22] R.G.S. Pala, H. Metiu, J. Phys. Chem. C 111 (2007) 8617–8622.
[23] H. Ohno, Science 281 (1998) 951–956.
[24] J.J. Wu, S.C. Liu, M.H. Yang, Appl. Phys. Lett. 85 (2004) 1027–1029.
[25] L. Liao, J.C. Li, D.F. Wang, C. Liu, M.Z. Peng, J.M. Zhou, Nanotechnology 17 (2006) 830–833.
[26] S. Wang, P. Li, H. Liu, J.B. Li, Y. Wei, J. Alloys Compd. 505 (2010) 362–366.
[27] X.Y. Zhou, S.H. Ge, D.S. Yao, Y.L. Zuo, Y.H. Xiao, J. Alloys Compd. 463 (2008) L9–L11.
[28] A. Mitra, R.K.T. Hareja, J. Appl. Phys. 89 (2001) 2025–2028.
[29] D.H. Zhang, Q.P. Wang, Z.Y. Xue, Appl. Surf. Sci. 207 (2003) 20–25.